Korea-Australia Rheology Journal
Vol. 19, No. 4, December 2007 pp. 191-199

A study of birefringence, residual stress and final shrinkage for precision injection molded parts

Sang Sik Yang[1] and Tai Hun Kwon[2*]

[1]Department of Mechanical Engineering Pohang University of Science and Technology, San 31, Hyojadong, Namgu, Pohang, Kyungbuk, 790-784, Republic of Korea*

(Received July 31, 2007)

Abstract

Precision injection molding process is of great importance since precision optical products such as CD, DVD and various lens are manufactured by those process. In such products, birefringence affects the optical performance while residual stress that determines the geometric precision level. Therefore, it is needed to study residual stress and birefringence that affect deformation and optical quality, respectively in precision optical product. In the present study, we tried to predict residual stress, final shrinkage and birefringence in injection molded parts in a systematic way, and compared numerical results with the corresponding experimental data.

Residual stress and birefringence can be divided into two parts, namely flow induced and thermally induced portions. Flow induced birefringence is dominant during the flow, whereas thermally induced stress is much higher than flow induced one when amorphous polymer undergoes rapid cooling across the glass transition region.

A numerical system that is able to predict birefringence, residual stress and final shrinkage in injection molding process has been developed using hybrid finite element-difference method for a general three dimensional thin part geometry. The present modeling attempts to integrate the analysis of the entire process consistently by assuming polymeric materials as nonlinear viscoelastic fluids above a no-flow temperature and as linear viscoelastic solids below the no-flow temperature, while calculating residual stress, shrinkage and birefringence accordingly. Thus, for flow induced ones, the Leonov model and stress-optical law are adopted, while the linear viscoelastic model, photoviscoelastic model and free volume theory taking into account the density relaxation phenomena are employed to predict thermally induced ones. Special cares are taken of the modeling of the lateral boundary condition which can consider product geometry, histories of pressure and residual stress. Deformations at and after ejection have been considered using thin shell viscoelastic finite element method. There were good correspondences between numerical results and experimental data if final shrinkage, residual stress and birefringence were compared.

keywords : precision injection molding, numerical simulation, birefringence, residual stress, shrinkage

1. Introduction

Although there have been various kinds of research for injection molded parts until now, one of challenging works was the investigation of residual stress and birefringence in injection molded parts. Recently, many optical injection molded products such as CD, DVD and various lenses have been developed and it is need to improve dimensional stability and optical quality. Many studies reported that residual stress and birefringence are key elements to determine the quality in such products. In particular, there have been many experimental and theoretical studies for residual stress because residual stress has direct influence on final shrinkage and warpage in injection molded parts.

During the entire injection molding process, the polymer undergoes development and relaxation of residual stress and birefringence while it is in fluid, rubbery and glassy states. During filling and packing stages, shear and normal stresses develop and relax or are frozen due to nonisothermal flow of the polymer. Such stresses due to flow are called as flow induced residual stress. On the other hand, large stress develops in stopped flow region when the polymer passes through a glass transition temperature during the rapid cooling stage. Under this circumstance, large mechanical modulus and long relaxation time of the polymer have large stress developed although it undergoes a small strain by temperature drop. Theses stress is referred to as thermally induced residual stress.

*Corresponding author: thkwon@postech.ac.kr

Several attempts have been made to theoretically predict flow induced residual stress and correlate it with frozen birefringence. Dietz and White (1978) have used the isothermal power-law model for flow in the core region with the subsequent nonisothermal stress relaxation simulated by means of a Maxwell-type model. Later, Greener and Pearson (1983) used the formulation of Dietz and White for the filling stage but introduced the nonisothermal stress relaxation according to the Marucci equation. Since the Leonov model is known to be successful to describe the viscoelastic behavior of polymer melts, the Leonov model (Leonov, 1976; Leonov *et al.*, 1976) has been employed as a nonlinear viscoelastic constitutive equation by many researchers in analyzing flow induced residual stress and birefringence. Isayev and Hieber (1980) studied flow induced residual stress and birefringence in a parallel plate during filling and cooling stages using the Leonov model. Baaijens (1991) analyzed residual stress in injection molding process including the packing stage in a rectangular plate. In particular, Baaijens applied the compressible Leonov model to the flowing region for flow induced residual stress and analyzed thermally induced residual stress in the solidified layer by appling the linearized Leonov model. Flaman (1993a; 1993b) presented the detailed analysis of injection molding process based on a compressible version of Leonov model to investigate flow induced birefringence for a thin strip cavity geometry. Friedrichs *et al.* (1996) predicted flow induced birefringence in a magneto-optical disk using the stress-optical law based on the incompressible Leonov model. Unfortunately, their evolution equations for elastic strain were not perfectly accurate for an axisymmetric coordinate system. Kim *et al.* (1999a; 1999b) numerically simulated the injection or injection/compression molding process including the compression process to predict flow induced birefringence and residual stress in a center-gated disk by employing the Leonov model with a correct tensor representation for an axisymmetric radial flow in a center-gated disk. However, the above mentioned works did not take into account thermally induced birefringence and residual stress.

Recently, many studies reported in the literature were concerned about thermally induced residual stress. Santhanam (1992) have predicted thermal residual stress in injection molded parts by introducing the linear viscoelastic model, but predicted residual stress was much higher than experimental result. Bushko and Stokes (1995a; 1995b) have studied thermal residual stress and shrinkage in solidification process of polymer materials between two parallel plates. But these studies did not take into account the density relaxation phenomena of polymeric materials in rapid cooling during the injection molding process. Based on the free volume theory, Shyu and Isayev (1995) and Shyu (1993) have developed the physical modeling to predict thermally induced birefringence and performed experimental measurements of it in free quenching samples. Also, Shyu and Isayev have predicted the birefringence including thermally induced portion in a center-gated disk, but have seemed not to consider an appropriate boundary condition for strain to predict thermally induced birefringence. Ghoneim and Hieber (1997) have attempted to predict thermal residual stress including density relaxation phenomena indicating that the density relaxation has significant effect on the evolution of residual stress. However, in their work, no attempt was made to compare numerical results with corresponding experimental ones. Lee and Kwon (2002a; 2002b) have developed a refined physical modeling based on the free volume theory, viscoelasticity and photoviscoelasticity and predicted residual stress and birefringence in the injection and injection/compression molded center-gated disk in a systematic manner. They reported that the boundary condition of strain shows a critical effect on the evolution of residual stress and density relaxation phenomena should be included to correlate numerical results with experimental data of birefringence. In addition, Lee and Kwon (2001) have extended their modeling to a general three-dimensional thin part based on a finite-element finite-difference hybrid scheme with control volume approach. They have validated developed system by comparing numerical results with corresponding ones from 2D approaches already developed by Lee and Kwon (2002a; 2002b).

The experimental approach for the residual stress in injection-molded parts has been employed in many works. In most of studies, the layer-removal method introduced by Treuting and Read (1951) has been utilized in evaluating the residual stress profile. Coxon and White (1979; 1980) investigated the effect of cross-linking on the residual stress in injection molded high density polyethylene and the effect of aging on the residual stress in injection-molded polyprolylene. Sandilands and White (1980) investigated the effect of injection pressure and crazing on the residual stress in molded bars of polystyrene using the layer removal method. Russell and Beaumont (1980) investigated the residual stress in nylon-6 injection-molded bars. According to them, the stress distribution in the molding is found to be parabolic with a compressive stress at the surface and a tensile stress at the center. Mandell *et al.* (1981) studied the residual stress in injection-molded polysurfone bars, particulary concerning its effect on fatigue. Siegmann *et al.* (1982) made an extensive study of the effect of injection-molding conditions on the residual stress in molded squares slabs from PPO(Noryl). Croutmal and Isayev (1984) have measured residual stress profiles in injection-molded specimens and observed that molding conditions played a vital role in the residual stress level in injection molded samples observed one year after the molding was performed. Hastenberg *et al.* (1992) have

measured the residual stress in injection molded flat plates with a modified layer-removal method. He has investigated effects of mold wall temperature and pressure history on the residual stress. Pham *et al.* (1993) have attempted to measure the residual stress in injection molded polycarbonate bars and have investigated effects of molding condition and molecular weights.

The experimental study of orientation in molded parts has been received considerable attention. Ballman and Torr (1960) measured the gapwise birefringence in injection-moded polystyrene strips and discovered the local maximum in the birefringence with zero values at the center and at the surface. Among numerous experimental investigations in this area, the work of Wales *et al.* (1972) is especially important since it involves the injection molding of materials having well characterized rheological properties. Also a few experimental studies (Flaman, 1993b; Isayev, 1983; Kamal and Tan, 1979) have investigated the birefringence distribution in injection-molded parts. In particular, Flaman (1993b) has measured the birefringence in a thin rectangular part according to various processing conditions. However, most studies have obtained the experimental data of either residual stress or birefringence for the injection molding process only.

2. Theory

The geometry of injection molded parts is considered as the assembly of thin flat plates. It is assumed that the molten core is surrounded by solidified outer layers and is gradually cooling down. A no-flow temperature is introduced to determine the region of solidified portions, and it is assumed to be T_g+30K. A non-linear viscoelastic liquid constitutive equation (Leonov, 1976) is applied above the no-flow temperature and a linear viscoelastic solid equation is applied below it (Lee and Kwon, 2002a; Lee and Kwon 2002b).

2.1. Filling, Packing and Cooling Stages

Governing equations such as continuity equation, linear momentum equations, energy equation with appropriate boundary conditions, constitutive equations and a state equation are completely described for filling, packing and cooling stages in (Lee and Kwon, 2002a; Lee and Kwon 2002b). Thus, the modeling of filling, packing and cooling stages is just briefly described in this section.

With the Hele-Shaw approximation, continuity and momentum equations are as follows:

$$\frac{\partial \rho}{\partial t}+\frac{\partial(\rho u)}{\partial x}+\frac{\partial(\rho v)}{\partial y}+\frac{\partial(\rho w)}{\partial z}=0, \tag{1}$$

$$0=-\frac{\partial p}{\partial x}+\frac{\partial \tau_{xz}}{\partial z}, \tag{2}$$

$$0=-\frac{\partial p}{\partial y}+\frac{\partial \tau_{yz}}{\partial z}, \tag{3}$$

$$0=-\frac{\partial p}{\partial z}+\frac{\partial \tau_{zz}}{\partial z}, \tag{4}$$

$$\rho c_p\left(\frac{\partial T}{\partial t}+u\frac{\partial T}{\partial x}+v\frac{\partial T}{\partial y}\right)=\frac{\partial}{\partial z}\left(k\frac{\partial T}{\partial z}\right)+\tau_{xz}\frac{\partial u}{\partial z}+\tau_{yz}\frac{\partial v}{\partial z}, \tag{5}$$

where ρ is the density, t the time, k the specific heat, c_p the thermal conductivity, p the pressure, T the temperature and u, v, w are velocity components in x, y, z directions and w is neglected in this flow situation.

As for boundary conditions, a no-slip boundary condition is applied along the mold wall. At the gate, constant flow rate in the filling stage, constant pressure in the packing stage and zero flow rate in the cooling stage are applied, respectively. Along the melt front, zero pressure is applied in the filling stage. For a thermal boundary condition, fixed mold wall temperature and convection boundary condition are assigned before and after ejection, respectively.

In the present study, the Leonov model was adopted as a nonlinear viscoelastic fluid model during the flow of polymeric liquid to predict flow induced residual stress and birefringence. The Leonov model can be expressed as below (Leonov, 1976; Leonov *et al.*, 1976),

$$\tilde{\tau}=2\eta_0 s\tilde{d}+\sum_{k=1}^{N}\frac{\eta_k}{\theta_k}\tilde{c}_k, \tag{6}$$

$$\tilde{c}_k^{\nabla}-\tilde{c}_k(\tilde{d}-\tilde{d}_k^p)-(\tilde{d}-\tilde{d}_k^p)\tilde{c}_k=0, \tag{7}$$

$$\tilde{d}_k^p=\frac{1}{\eta_k}\left[\left(\tilde{c}_k-\frac{I_{k,1}}{3}\tilde{I}\right)-\left(\tilde{c}_k^{-1}-\frac{I_{k,2}}{3}\tilde{I}\right)\right], \tag{8}$$

where $\tilde{\tau}$ is the stress tensor except isotropic pressure term, $\tilde{d}$ is the rate of deformation tensor, s is the rheological parameter ranging between zero and unity, $\tilde{c}_k$ is the k-th mode Finger strain tensor representing the elastic deformation of polymeric material. Also η_k and θ_k are, respectively, the viscosity and the relaxation time of k-th mode. And $\tilde{d}_k^p$ is an irreversible rate of deformation tensor, I_1, I_2 are basic invariants of Finger strain tensor and $(\,)^{\nabla}$ signifies the upper convected derivative. In addition, to express constitutive equations dependent on temperature change and deformation history, WLF shift factor was employed to η_k, θ_k based on the thermo-rheological simplicity concept (Isayev, 1987; Famili and Isayev, 1991).

$$\eta_k(T)=\eta_k(T_0)\frac{a_T}{a_{T_0}}, \tag{9}$$

$$\theta_k(T)=\theta_k(T_0)\frac{a_T}{a_{T_0}}, \tag{10}$$

$$a_T=\begin{cases} a_{T_g} & \text{if} \quad T\le T_g, \\ \exp\left[-\dfrac{c_1(T-T_{ref})}{c_2+(T-T_{ref})}\right] & \text{if} \quad T>T_g. \end{cases} \tag{11}$$

To consider the compressibility in the packing stage, the Tait equation was used to define the density (ρ) and its change with respect to temperature (T) and pressure (p) as

follows (Chiang *et al.*, 1991a; Chiang *et al.*, 1991b; Chiang *et al.* 1993).

$$\rho(T,p)=\rho_0(T)\left\{1-0.0894\ln\left[1+\frac{p}{B(T)}\right]\right\}^{-1}, \tag{12}$$

where

$$\frac{1}{\rho_0(T)}=\begin{cases}b_{1,l}+b_{2,l}(T-b_5), T>T_g(p),\\ b_{1,s}+b_{2,s}(T-b_5), T\le T_g(p),\end{cases} \tag{13}$$

$$B(T)=\begin{cases}b_{3,l}+\exp(-b_{4,l}T), T>T_g(p),\\ b_{3,s}+\exp(-b_{4,s}T), T\le T_g(p),\end{cases} \tag{14}$$

$$T_g(p)=b_5+b_6p. \tag{15}$$

Meanwhile, when the polymeric material is above the glass transition temperature the stress-optical law can be applied to the polymer (White, 1991; Janeschitz-Kriegl, 1983), namely

$$n_i-n_j=C(\sigma_i-\sigma_j), \tag{16}$$

where C is the stress-optical coefficient, n_i the refractive index, and σ_i the principal stress.

2.2. Free Volume Theory

Injection molded products experience rapid temperature change by far lower temperature of the mold wall than melt temperature, which results in a non-equilibrium density response. It is assumed that the non-equilibrium density response could be expressed by first order differential equation (Shyu and Isayev, 1995) in terms of free volume.

$$\frac{d\delta}{dt}=-\frac{\delta}{\tau}-\Delta\alpha\frac{dT}{dt}, \tag{17}$$

where δ is the fractional free volume defined as

$$\delta=\frac{V(t)-V_\infty(T,p)}{V_{ref}}. \tag{18}$$

V, V_∞ and V_{ref} represent the specific volumes at current time t, equilibrium, and that of the reference temperature, respectively. $\Delta\alpha=\alpha_l-\alpha_s$ is the thermal expansion coefficient difference between liquid and solid states. $\tau=\tau_0 a_T$ is the relaxation time of the free volume at temperature T. An effective temperature represents the non-equilibrium density state as a function of the free volume and is defined in equation (19).

$$T_{eff}=T+\frac{\delta}{\Delta\alpha}. \tag{19}$$

2.3. Thermally Induced Birefringence and Residual Stress

As mentioned before, it is assumed that the change of the stress occurs in the thickness direction and the molten core is surrounded by solidified outer layers. The polymer is assumed to have the thermorheological simplicity, therefore time temperature equivalence holds through a shift function, which has the WLF type in the high temperature and the Arrhenius type in the low temperature:

$$\mu_T(t)=\mu_{Tr}(tf(T)), \tag{20}$$

$$\frac{1}{f(T)}=a_T=\begin{cases}\exp\left[-\frac{A_1(T-T_r)}{A_2+T-T_r}\right], & if\quad T>T_g-20,\\ \exp[A_3-A_4(T-273)], & if\quad T\le T_g-20.\end{cases} \tag{21}$$

In the modeling of solidified polymer, the linear viscoelastic solid behavior is assumed for a deviatoric part and the elastic solid behavior for a dilatational part and the photoviscoelasticity is used to calculate thermally induced birefringence.

$$s_{ij}=\int_0^\xi 2\mu(\xi-\xi')\frac{\partial e_{ij}}{\partial\xi'}d\xi', \tag{22}$$

$$\sigma_{ii}=3K(\varepsilon_{ii}-3\alpha_0\Theta), \tag{23}$$

$$n_{ij}=n_{oij}+\int_0^\xi O(\xi-\xi')\frac{\partial e_{ij}}{\partial\xi'}d\xi', \tag{24}$$

where σ_{ij}, ε_{ij} represent Cauchy's stress and strain tensors, respectively. s_{ij}, e_{ij} are deviatoric parts of stress and strain, respectively. It may be noted that n_{oij} is the initial refractive tensor. The material time and the thermal expansion coefficient are defined in terms of the effective temperature so that the structural relaxation phenomena can be considered as below:

$$\xi=\int_0^t f(T_{eff})dt'=\int_0^t\frac{1}{a_T(T_{eff})}dt', \tag{25}$$

$$\Theta=\frac{1}{\alpha_0}\int_{T_0}^{T_{eff}}\alpha(T')dT'. \tag{26}$$

It is known that if the shear modulus is expressed by equation (27) using the Prony series, which is linear combinations of decaying exponentials, the time increment formula of stress can be simplified into the function of the current time and the previous time only through the recurrent formulation.

$$\mu(\xi)=\mu_0+\sum_{i=1}^{n}\mu_i e^{-\xi/\tau_i}. \tag{27}$$

2.4. Lateral Boundary Condition considering In-plane Constraint and Sticking Effect

Appropriate modelings for the boundary condition are needed to consider effects of the complex geometry of the mold and the interaction between molded part and mold wall. In this study, we considered the in-plane constraint by the complex geometry of the mold and sticking effect.

If there is in-plane constraint, the deformation in that direction is not allowed until ejection. In other words, if the direction x is constrained by the in-plane constraint, $\Delta\varepsilon_{xx}=0$. If there is no in-plane constraint, sticking model

is applied. In this case, two types of boundary conditions have been adopted as extreme cases. One is prohiviting any deformation until ejection, as shown in (28), the other is allowing sliding to satisfy force free condition right after the pressure falls to zero as shown in (29),

$$\Delta\varepsilon_{xx} = 0\,, \tag{28}$$

$$\int_0^b \sigma_{xx}(z)dz = 0\,. \tag{29}$$

From now on, the former will be called as a no slip model and the latter as a free slide model.

Sticking model can express not only both models but also intermediate regions between two extremes. Developed model in this study determines the moment of the transition of boundary condition from (28) to (29) by comparing averaged lateral stress with sticking parameter S_{tr}. Sticking off criterion is as follows:

- ▷ Until averaged lateral stress is smaller than sticking parameter(S_{tr}), the part is not allowed to shrink in lateral direction.
- ▷ If averaged lateral stress gets larger than S_{tr}, the part is free to shrink.

2.5. Deformation Analysis at and after Ejection

A thin-shell structural finite element analysis system is developed to determine the displacement by the stress and strain conditions. Under small deformation, it is possible to treat the shell element as an assembly of a membrane element and a plate bending element. In this study, we have employed Bergan's membrane element which uses the rotational degree of freedom to describe the deformation of the membrane element (Bergan and Felippa, 1985) and Batoz's Discrete Kirchhoff Triangle element (Batoz et al., 1980). The deformation of the shell is assumed as a sum of the membrane deformation that represents the averaged deformation in the in-plane direction and the plate bending deformation that represents the out-of-plane deformation. Because the plate is thin, it is assumed that the plate is in the plane stress state (σ_{zz}=0) and the effect of the shear stress (τ_{xz}, τ_{yz}) is neglected.

The product is assumed as an elastic material at ejection. During the ejection process, the redistribution of residual stress almost instantaneously occurs as the boundary condition changes, resulting in an instantaneous deformation since the ejection process has rather short time interval. In the analysis of elastic deformation, the resultant stress and the resultant moment are regarded as an initial stress and an initial moment. The deformation occurred inside the mold are also considered as an initial strain.

In calculating the out-of-mold deformation, thermoviscoelastic model is adopted. The time discretization (Kaliske and Rothert, 1997) between material times ξ^n and ξ^{n+1} can be obtained using the equations (22), (23), (27).

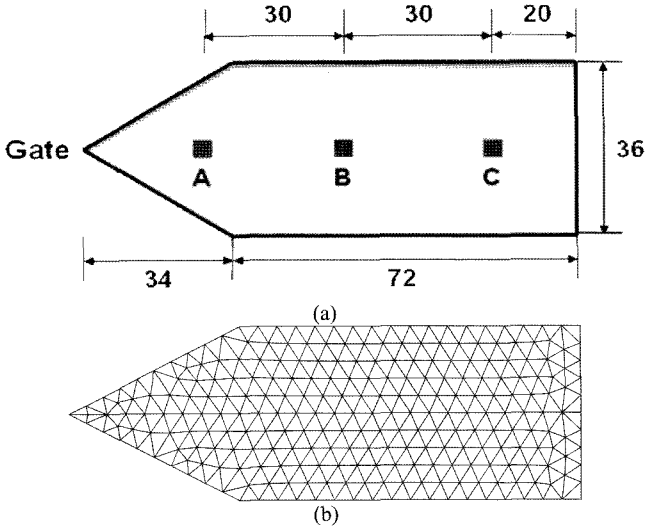

Fig. 1. (a) Geometry of a flat plate and selected positions and (b) the corresponding finite element mesh.

$$\Delta\sigma_{ij}^n = \left(K - \frac{2}{3}\mu_0 - \sum_{p=1}^{N}\frac{2\mu_p}{3}\frac{1-e^{-\Delta\xi^n/\tau_p}}{\Delta\xi^n/\tau_p}\right)\Delta\varepsilon_{kk}^n\delta_{ij} +$$

$$+\left(2\mu_0 + \sum_{p=1}^{N} 2\mu_p\frac{1-e^{-\Delta\xi^n/\tau_p}}{\Delta\xi^n/\tau_p}\right)\Delta\varepsilon_{ij}^n + K\varepsilon_{kk}^n\delta_{ij} + 2\mu_0\left(\varepsilon_{ij}^n - \frac{1}{3}\varepsilon_{kk}^n\delta_{ij}\right) - \sigma_{ij}^n$$

$$+\sum_{p=1}^{N} e^{-\Delta\xi^n/\tau_p}h_{ij(p)}^n - 3K\alpha_0\Delta\Theta^n\delta_{ij} - 3K\alpha_0\Delta\Theta^n\delta_{ij}\,, \tag{30}$$

where $h_{ij(p)}^n$ is the p-th mode viscous stress and decaying as following manner;

$$h_{ij(p)}^n = \int_0^{\xi^n} 2\mu_p e^{-(\xi^n - s)/\tau_p}\frac{\partial}{\partial s}(e_{ij}(s))ds\,. \tag{31}$$

Equations (30), (31) with proper initial conditions are applied on structural FEM to obtain the stress and strain differences.

3. Experimental

In the experiment, the shrinkage of injection molded PS(Dow Chemical Styron 615APR-W) square flat plate was measured. The Sumitomo SE50D, the injection molding machine is used to product samples with fully dried pellets. Two mold geometries, a square flat plate and one with two side walls, were tested to verify the effect of the in-plane constraint from the mold geometry (Fig. 2). The dimension of the square flat plate has length of 3.5cm and thickness of 0.2 cm. The height of side walls is 0.3cm and its thickness is 0.2 cm. 10 samples were measured by the combination of the micrometer attached single axis stage and the optically zoomed CCD. Measurement was performed one day after molding.

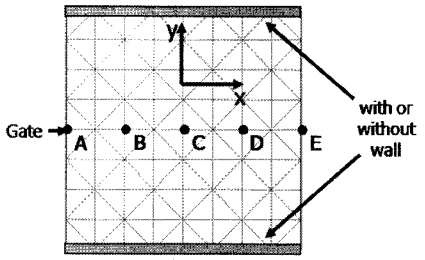

Fig. 2. Geometry of a square flat plate and selected positions and finite element mesh.

Table 1. Processing conditions

Geometry	Flat plate	Square flat plates
Flow rate or filling time	7.5 cm^3/sec	0.2 sec
Packing pressure	16.5 MPa	10 MPa
Packing time	10 sec	5 sec
Melt temperature	220 °C	230 °C
Wall temperature	40 °C	40 °C

4. Results and Discussion

4.1. Geometry and Mesh

Three test geometries were selected. Fig. 1 shows a flat plate. Thickness of the flat plate is 0.2 cm. Unit in the Fig. 1 is mm. Three points are selected to display gapwise distributions of birefringence and residual stress. Fig. 2 shows geometries and meshes of the square flat plate which are tested in the simulation and experiment. The existence of walls in the y direction determines the existence of the in-plane constraint. The gate is located at the middle of left side of the part.

4.2. Processing Conditions

Table 1 designates processing conditions. Processing conditions for the flat plate and square flat plates are chosen differently. In the flat plate, calculated birefringence and residual stress distribution were compared with experimental result in the literature (Hastenberg *et al.*, 1992). In square flat plates, calculated shrinkages are compared with experimental data performed in this study.

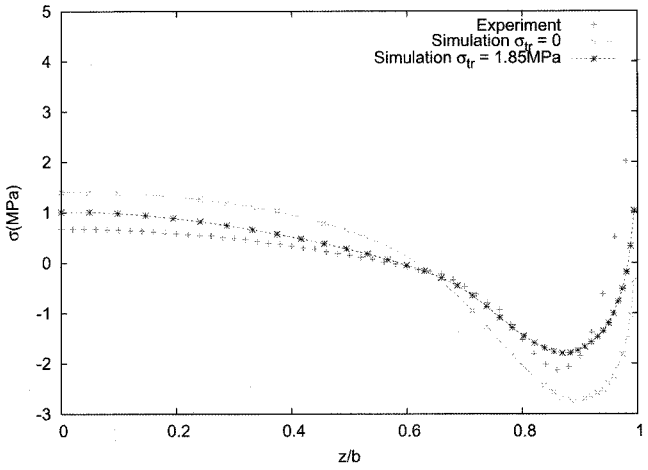

Fig. 4. Distributions of residual stress at point B.

4.3. Birefringence and Residual Stress Distribution of the Flat Plate

The predicted distribution of birefringence and residual stress are compared with the corresponding experimental data in Fig. 3. Fig. 3(a) shows the comparison between experimental data and numerical results from free slide model. It may be noted that the birefringence results including sticking model are omitted since results are almost same. With respect to the distribution of birefringence, the overall shape of numerical results is in good agreement with that of experimental data. However, the prediction underestimates the peak of the birefringence of experimental data especially at the position of A. Fig. 4 shows distributions of residual stresses from experiment, calculated with free slide model and with sticking model. Calculated residual stresses profiles are in good agreement with experimental data in overall shape, in that tensile stress in the core and compressive stress in the intermediate zone. And result from sticking model is closer to experimental data than free slide model. Therefore, it can be said

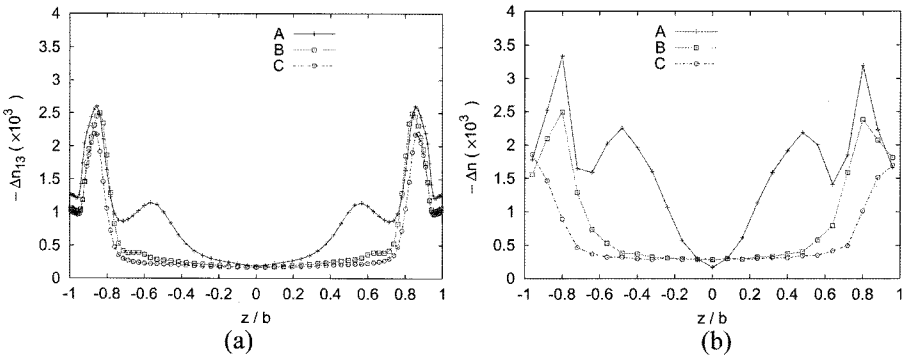

Fig. 3. Distributions of calculated (a) and measured (b) birefringence.

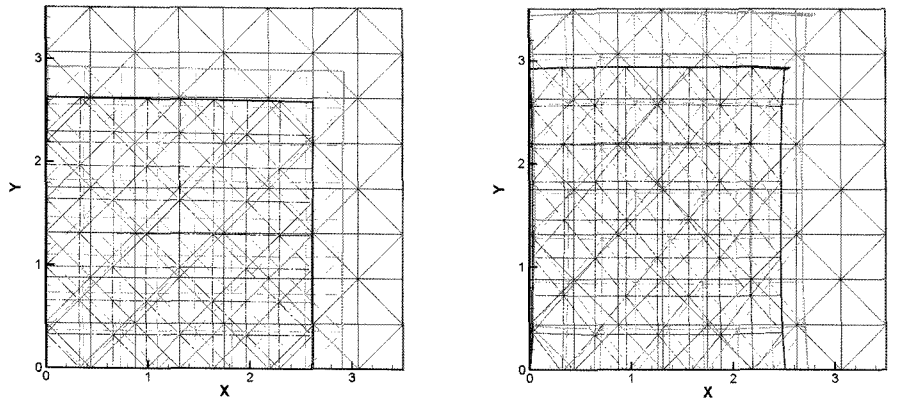

(a) Square plate (b) square plate with two side walls

Fig. 5. Original shape (solid), deformed shape after ejection (dashed) and at equilibrium (dashed dot dot), deformation is 30 times magnified.

that the sticking model predicts final shrinkage and residual stress more closely to the measured ones while it affects birefringence little.

4.4. The Effect of In-Plane Constraint on Shrinkage

Fig. 5 represents calculated shrinkages just after ejection and at equilibrium. In the case of no in-plane constraint (Fig. 5(a)), it showed little difference between x and y directions. However, if there is in-plane constraint due to side walls located in upper and lower sides, the shrinkage in the constrained direction was considerably smaller than that in unconstrained direction. However, predicted shrinkage was smaller than measured one by about 16%(Fig. 6).

4.5. Determination of Parameters for Sticking Model

To utilize sticking model in the calculation of residual stress, it is necessary to determine a parameter. The parameter was selected to match the final shrinkage by the experiment. As shown in Fig. 7, determined value was 1.85 MPa. It is noted that by changing parameters it is convenient to change from free slide to no slip models. For example, $S_{tr}=0$, $S_{tr}=\infty$ correspond to free slide and no slip models, respectively.

5. Conclusion

In this study, we have developed the injection molding analysis system to predict residual stresses, final shrinkage and birefringence for a thin three-dimensional injection molded parts. Two sets of physical modeling were introduced depending on the material state: a liquid state above a no-flow temperature is described by a nonlinear viscoelastic fluid model, specifically the Leonov model and a stress-optical law; a solid state below the no-flow tem-

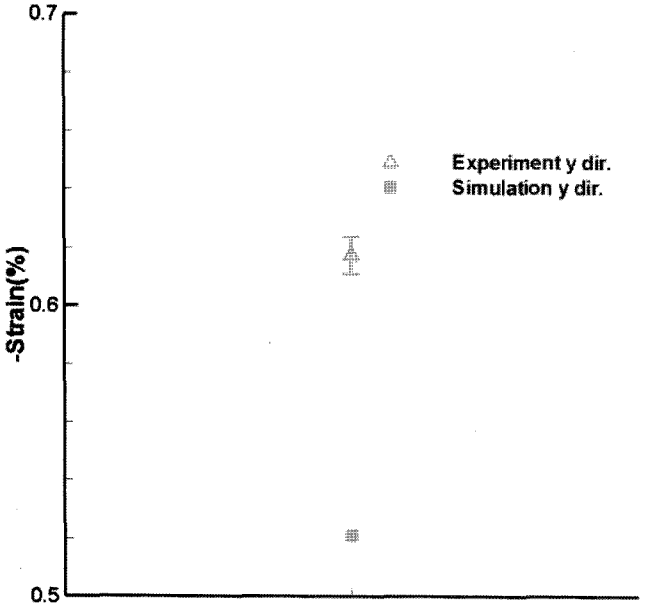

Fig. 6. Comparison of the shrinkage in the constrained direction due to in-plane constraint.

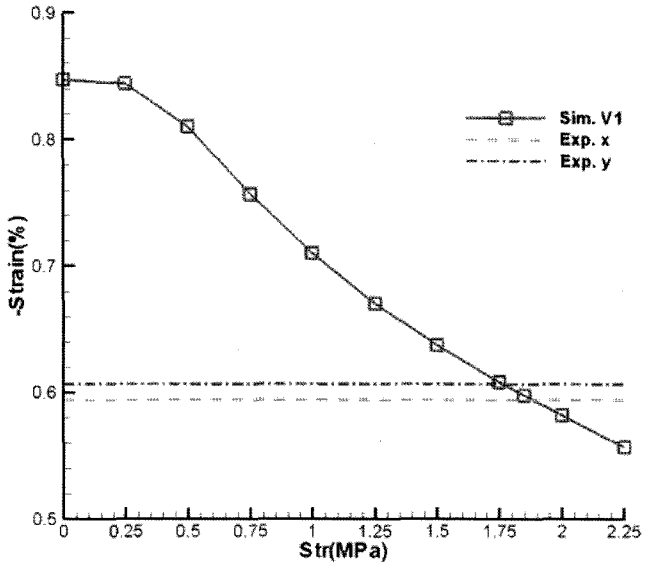

Fig. 7. Determination of sticking parameter S_{tr}.

perature is described by a linear viscoelastic solid model, a photoviscoelastic model and the free volume theory taking into account the density relaxation phenomena. Special cares were taken of the lateral boundary condition from the in-plane constraint due to a complex geometry and from the sticking effect based on the interaction between polymer and mold wall. For the validation of a developed system, we have applied the system to a flat plate and square flat plates. The following conclusions according to our numerical study were obtained. With respect to the distribution of birefringence, the overall shape of numerical results is in good agreement with that of experimental data. With respect to the distribution of residual stress, calculated profiles are in good agreement with experimental data in overall shape, and calculated results with the sticking model were closer to the experimental results. By considering in-plane constraint, much smaller shrinkage was predicted in the constrained direction than that in unconstrained. However, it predicted smaller shrinkage than experimental one. By introducing sticking model, more precise prediction of shrinkage was possible.

Acknowledgements

I appreciate the support of Defense Acquisition Program Administration and Agency for Defense Development for this study to be completed under the contract UD060049-AD and also appreciate the Korean Ministry of Commerce, Industry and Energy for financial support *via* the research project of the National RND program(NM5410).

References

Baaijens, F. P. T. 1991, Calculation of residual stresses in injection molded products, Rheol. Acta **30**, 284-299.

Ballman, R. L. and H. L. Torr, 1960, Modern Plastics **38**, 113.

Batoz, J. L., K. J. Bathe and L. W. Ho, 1980, Study of three-node triangular plate bending elements, International Journal for Numerical Methods in Engineering **15**, 1771-1812.

Bergan, P. G. and C. A. Felippa, 1985, Triangular membrane element with rotational degrees of freedom, *Computer Methods in Applied Mechanics and Engineering* **50**, 25-69.

Bushko, W. C. and V. K. Stokes, 1995a, Solidification of thermoviscoelastic melts. part I: formulation of model problem, Polym. Eng. Sci. **35**, 351-364.

Bushko, W. C. and V. K. Stokes, 1995b, Solidification of thermoviscoelastic melts. part II: effects of processing conditions on shrinkage and residual stresses. Polym. Eng. Sci. **35**, 365-384.

Chiang, H. H., C. A. Hieber and K.K. Wang, 1991a, A nuified simulation of the filling and postfilling stages in injection molding. part I: formulation, Polym. Eng. Sci. **31**, 116-124.

Chiang, H. H., C. A. Hieber and K.K. Wang, 1991b, A nuified simulation of the filling and postfilling stages in injection molding. part II: experimental verification, Polym. Eng. Sci. **31**, 125-139.

Chiang, H. H., K. Himasekhar, N. Santhanam and K. K. Wang, 1993, Integrated simulation of fluid flow and heat transfer in injection molding for the prediction of shrinkage and warpage, J. Eng. Mat. And Tech. **115**, 37-47.

Coxon, L. D. and J. R. White, 1979, Measurement of internal stresses in chemically cross-linked high-density polyethylene, J. Mater. Sci. **14**, 1114-1120.

Coxon, L. D. and J. R. White, 1980, Residual stresses and aging in injection molded polypropylene, Polym. Eng. Sci. **20**, 230-236.

Dietz, W. and J. L. White, 1978, Ein einfaches Modell zur Berechnung des Druckverlustes wahrend des Werkzeugfullvorganges und der eingefrorenen Orientierung beim Spritzgießen amorpher Kunststoffe, Rheol. Acta **17**, 676-692.

Flaman, A. A. M., 1993a, Buildup and relaxation of molecular orientation in injection molding. part I: formulation, Polym. Eng. Sci. **33**, 193-201.

Flaman, A. A. M., 1993b, Buildup and relaxation of molecular orientation in injection molding. part II: experimental verification, Polym. Eng. Sci. **33**, 202-210.

Friedrichs, B., M. Horie and Y. Yamaguchi, 1996, Simulation and analysis of birefringence in magneto-optical discs. part A: formulation, J. Materials Processing & Manuf. Sci. **5**, 95-113.

Ghoneim H. and C. A. Hieber, 1997, Incorporation of density relaxation in the analysis of residual stresses in molded parts, Polym. Eng. Sci. **37**, 219-227.

Greener, J. and G. H. Pearson, 1983, Orientation residual stresses and birefringence in injection molding, J. Rheol. **27**, 116-134.

Hastenberg, C. H. V., P. C. Wildervanck, A. J. H. Leenen and G. G. J. Schennink, 1992, The measurement of thermal stress distributions along the flow path in injection-molded flat plates, Polym. Eng. Sci. **32**, 506-515.

Isayev, A. I. and C. A. Hieber, 1980, Toward a viscoelastic modelling of the injection molding of polymers, Rheol. Acta **19**, 168-182.

Isayev, A. I., 1983, Orientation development in the injection molding of amorphous polymers, Polym. Eng. Sci. **23**, 271-284.

Isayev, A. I. and D. L. Crouthamel, 1984, Residual stress development in the injection molding of polymers, Polymer-plastics technology and engineering **22**, 177-232.

Janeschitz-Kriegl, H., 1983, Polymer melt rheology and flow birefringence, Springer-Verlag, Berlin.

Kaliske, M. and R. Rothert, 1997, Formulation and implementation of three-dimensional viscoelasticity at small and finite strains, Computational Mechanics **19**, 228-239.

Kamal, M. R. and V. Tan, 1979, Orientation in injection molded polystyrene, Polym. Eng. Sci. **19**, 558-563.

Famili, N. and A.I. Isayev, 1991, *Modeling of Polymer Processing*, Hanser Publisher, New York.

Kim, I. H., S. J. Park, S. T. Chung and T. H. Kwon, 1999a, Numerical modeling of injection/compression molding for center-gated disk: part I: injection molding with viscoelastic compressible fluid model, Polym. Eng. Sci. **39**, 1930-1942.

Kim, I. H., S. J. Park, S. T. Chung and T. H. Kwon, 1999b, Numerical modeling of injection/compression molding for center-gated disk: part II: effect of compression stage, Polym. Eng.

Sci. **39**, 1943-1951.

Lee, Y. B. and T. H. Kwon, 2002a, Numerical prediction of residual stresses and birefringence in injection/compression molded center-gated disk. part I: basic modeling and results for injection molding, Polym. Eng. Sci. **42**, 2246-2272.

Lee, Y. B. and T. H. Kwon, 2002b, Numerical prediction of residual stresses and birefringence in injection/compression molded center-gated disk. part II: Effects of processing conditions, Polym. Eng. Sci. **42**, 2273-2292.

Lee, Y. B. and T. H. Kwon, 2001, PPS 17th Annual meeting, PPS-17.

Leonov, A. I., 1976, Nonequilibrium thermodynamics and rheology of viscoelastic polymer media, Rheol. Acta **15**, 85-98.

Leonov, A. I., E. H. Lipkina, E. D. Paskhin and A. N. Prokunin, 1976, Theoretical and experimental investigation of shearing in elastic polymer, Rheol. Acta **15**, 411-426.

Mandell, J. F., K. L. Smith and D. D. Huang, 1981, Effects of residual stress and orientation on the fatigue of injection molded polysulfone, Polym. Eng. Sci. **21**, 1173-1180.

Pham, H. T., C. P. Bosnyak and K. Sehanobish, 1993, Residual stresses in injection molded polycarbonate rectangular bars, Polym. Eng. Sci. **33**, 1634-1643.

Russell, D. P. and P. W. R. Beaumont, Structure and properties of injection-moulded nylon-6 - part 2 residual stresses in injection-moulded nylon-6, J. Mater. Sci., **15**, 208-215.

Santhanam, N., 1992, PhD thesis, Cornell university, Ithaca, N.Y.

Sandilands, G. J. and J. R. White, 1980, Effect of injection pressure and crazing on internal stresses in injection-moulded polystyrene, Polymer **21**, 338-343.

Shyu, G. D. and A. I. Isayev, 1995, Residual stresses and birefringence in injection molded disks, SPE ANTEC Tech. Papers **41**, 2911-2917.

Shyu, G. D., 1993, PhD thesis, The university of Akron.

Siegmann, A., A. Buchman and S. Kenig, 1982, Residual stresses in polymers - 3. the influence of injection-molding process conditions, Polym. Eng. Sci. **22**, 560-568.

Treuting, R. G. and W. T. Read Jr., 1951, A mechanical determination of biaxial residual stress in sheet materials, J. Appl. Phys. **22**, 130-134.

Wales, J. L. S., Ir J. Van Leeuwen and R. Van Der Vijgh, 1972, Some aspects of orientation in injection molded objects, Polym. Eng. Sci. **12**, 358-363.

White, J. L., 1991, Principles of polymer engineering rheology, John Wiley & Sons, New York.